200 Gbps/lane IM/DD Technologies for Short Reach Optical Interconnects

Citation for the original published paper (version of record):

Pang, X., Ozolins, O., Lin, R. et al (2020). 200 Gbps/lane IM/DD Technologies for Short Reach Optical Interconnects. Journal of Lightwave Technology, 38(2): 492-503.
http://dx.doi.org/10.1109/JLT.2019.2962322

200 Gbps/lane IM/DD Technologies for Short Reach Optical Interconnects

Xiaodan Pang, *Senior Member, IEEE, Member, OSA*, Oskars Ozolins, *Member, IEEE,*
Rui Lin, *Member, IEEE,* Lu Zhang, *Student Member, IEEE,* Aleksejs Udalcovs, *Member, IEEE,*
Lei Xue, Richard Schatz, Urban Westergren, *Member, IEEE,* Shilin Xiao, *Member, IEEE,*
Weisheng Hu, *Member, OSA*, Gunnar Jacobsen, Sergei Popov, *Member, IEEE, Fellow, OSA,* and
Jiajia Chen, *Senior Member, IEEE, Member, OSA*

***Abstract*—Client-side optics are facing an ever-increasing upgrading pace, driven by upcoming 5G related services and datacenter applications. The demand for a single lane data rate is soon approaching 200 Gbps. To meet such high-speed requirements, all segments of traditional intensity modulation direct detection (IM/DD) technologies are being challenged. The characteristics of electrical and optoelectronic components, and the performance of modulation, coding and digital signal processing (DSP) techniques are being stretched to their limits. In this context, we witnessed technological breakthroughs in several aspects, including development of broadband devices, novel modulation formats and coding, and high-performance DSP algorithms for the past few years. A great momentum has been accumulated to overcome the aforementioned challenges. In this paper, we focus on IM/DD transmissions, and provide an overview of recent research and development efforts on key enabling technologies for 200 Gbps per lane and beyond. Our recent demonstrations of 200 Gbps short-reach transmissions with 4-level pulse amplitude modulation (PAM) and discrete multitone signals are also presented as examples to show the system requirements in terms of device characteristics and DSP performance. Apart from digital coherent technologies and advanced direct detection systems, such as Stokes-vector and Kramers-Kronig schemes, we expect high-speed IM/DD systems will remain advantageous in terms of system cost, power consumption and footprint for short reach applications in the short- to mid- term perspective.**

***Index Terms*—Optical fiber communication, optical interconnections, intensity modulation direct detection, digital signal processing.**

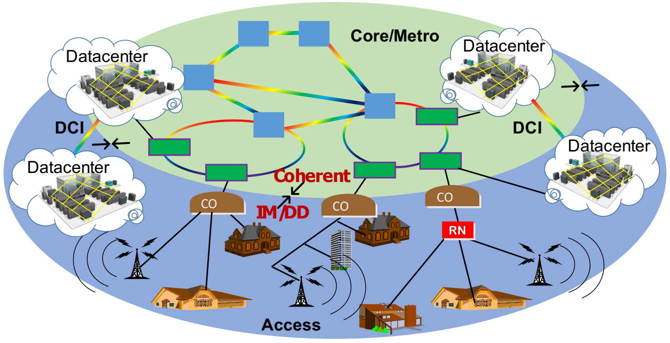

Fig. 1. A typical core, metro and access network scenario, including the metro-edge and intra-/inter-datacenter links, where the high-speed IM/DD links are required. CO: center office; RN: remote node; DCI: datacenter interconnects.

I. INTRODUCTION

INTENSITY modulation direct detection (IM/DD) technology had been the dominating solution in all segments of fiber-optic communication networks since its first generation. However, approximately one decade ago, transceivers based on the digital coherent optical technology were demonstrated and developed [1], and have quickly replaced the IM/DD solutions in many scenarios, in particular, the core/metro segments. To date, there has been a continuous process of upgrading fiber-optic networks from the legacy 10 Gbps systems to 100/200 Gbps, and soon 400 Gbps coherent based solutions on the line side for long-haul and metro networks, following the requirements of telecommunication carriers [2]. Together with

Manuscript received on June 21, 2019, revised on November xx, 2019. This work is supported in part by the European Commission through H2020-MCSA-IF NEWMAN Project under Grant 752826, in part by the SJTU State Key Laboratory of Advanced Optical Communication System and Networks Open Project 2018GZKF03001, in part by the Swedish Research Council (VR) project 2016-04510 "PHASE", 2016-04489 "Go-iData", the Swedish ICT–TNG project SCENE, Swedish Foundation for Strategic Research (SSF), Göran Gustafsson Foundation, Vinnova-funded Celtic Plus sub-projects C2015/3-5 SENDATE-FICUS and SENDATE-EXTEND, and Vinnova project 2017-01559 "Centre for Software-Defined optical networks" *(Xiaodan Pang and Oskars Ozolins contributed equally to this work, corresponding author: Jiajia Chen.)*

X. Pang is with Global R&D of Infinera Corporation, Stockholm 117 43, Sweden and the Kista High Speed Transmission Lab, KTH Royal Institute of Technology, Kista 164 40, Sweden (e-mail: xiaodan@kth.se).

O. Ozolins, A. Udalcovs and Gunnar Jacobsen are with the NETLAB, RISE AB, Kista SE-164 25, Sweden. O. Ozolins is also an affiliated faculty on optical communication at KTH. Royal Institute of Technology (e-mails: oskars.ozolins@ri.se; aleksejs.udalcovs@ri.se, gunnar.jacobsen@ri.se).

R. Lin, L. Xue and J. Chen are with the Electrical Engineering Department, Chalmers University of Technology, SE-412 96 Gothenburg (ruilin@chalmers.se, leixu@chalmers.se, jiajiac@chalmers.se).

L. Zhang is with the State Key Laboratory of Advanced Optical Communication System and Networks, Shanghai Jiao Tong University, Shanghai 200240, China and College of Information Science and EE, Zhejiang University, Hangzhou 310027, China (email: luzhang_sjtu@sjtu.edu.cn).

S. Xiao and W. Hu are with the State Key Laboratory of Advanced Optical Communication System and Networks, Shanghai Jiao Tong University, Shanghai 200240, China (email: slxiao@sjtu.edu.cn, wshu@sjtu.edu.cn).

R. Schatz, U. Westergren and S. Popov are with the Applied Physics Department, KTH Royal Institute of Technology (rschatz@kth.se, urban@kth.se, sergeip@kth.se).

the demand of 5G related applications from the access networks, such upgrades push the data rate of IM/DD based client side optics to match the transponder speed on the line side by supporting 400 Gbps capacity and beyond [3]. Besides such a continuous evolution of traditional telecom networks, a more demanding scenario for IM/DD interfaces with a higher date rate has recently been driven by the content providers, who often have their own network infrastructure in the form of datacenters [4]. Nowadays, datacenters experience an enormous traffic growth due to the vast amount of data to be stored, transmitted and processed. These high-speed data links can be divided into two groups: intra datacenter links and datacenter interconnects (DCI). The first group are the short reach high-speed data links covering distances ranging from a few meters to a few kilometers, which connect servers and racks inside the datacenters. The DCI links enable data exchange among multiple datacenters with much longer distances compared with intra datacenter links, normally in the scale from a few kilometers up to a few hundred kilometers [5]. Various industrial standards and multi-source agreement (MSA) groups are established to propose transceiver specifications for these application scenarios [6]-[8]. For example, regarding the supported distances, the 100 Gigabit Ethernet (100GbE) transceiver standards can be categorized into short reach (SR) segment, supporting up to 100 m OM4 multimode fiber (MMF) links; datacenter reach (DR), supporting up to 500 m single mode fiber (SMF) links; fiber reach (FR) for up to 2 km SMF, long reach (LR) for up to 10 km SMF; and extended reach (ER), to offer up to 40 km SMF. For the upcoming 400G era and beyond, IM/DD solutions are still prioritized for these specifications due to their advantages in terms of cost, power consumption, and footprint [9]-[11].

Figure 1 shows a typical core, metro and access network scenario, covering most of the application areas where high-speed IM/DD links are required. Currently, the boundary separating the digital coherent solutions and IM/DD based solutions exists arguably between the metro and access network segments. However, this boundary will become less clear in the 400G era and beyond. Both technical and economic challenges arise to keep up with the bandwidth growth for the IM/DD technologies. Meanwhile, low-cost digital coherent based solutions are proposed and developed to cover medium to short reach applications, e.g. the 400G ZR solution which can be packed into a QSFP-DD-DCO (Quad Small Form Factor Pluggable Interface Double Density Digital Coherent Optics) or an OSFP (Octal SFP)-DCO form factor, to enable a dense wavelength division multiplexing (DWDM) link up to 120 km [12].

Concerning post 400G-era solutions, enormous challenges for both digital coherent and IM/DD technologies are foreseen. Currently, research and development efforts are put in many different aspects, including components, modulation formats and digital signal processing (DSP) techniques, to meet the speed, cost, power consumption and footprint requirements [13]. The digital coherent transceivers are mainly facing engineering challenges to simplify high performance versions, which are used for core networks in order to adapt to short reach application requirements. Meanwhile, conventional IM/DD technologies are facing more fundamental challenges to meet the bitrate requirement. Unlike coherent technologies, which utilize all dimensions of freedom of an optical carrier (amplitude, phase and polarization) to carry data, only the amplitude is used in the IM/DD systems. Therefore, an underlying trade-off between the data rate per lane and number of lanes becomes important for consideration. While utilizing more parallel lanes can increase the supported data rate linearly, there are always a limited number of lanes one can pack into an optical transceiver, given the footprint, power consumption and cost constraints. Therefore, in the context of 400G (and beyond) client optics, many efforts are devoted on tackling the challenge to increase the data rate per lane.

Currently, broadband electrical and optoelectronic components are being designed and developed to facilitate high bandwidth modulations. Advanced modulation formats with powerful DSP and coding techniques are proposed and implemented to optimize the spectral efficiency and transmission performance. Combining these advanced techniques, many system-level demonstrations of over 100 Gbps per lane transmissions have been reported. It shows a promising progress towards maturity for industrial development, where 200 Gbps per lane is the nearest target. Besides the digital coherent and the traditional IM/DD solutions, there are many hybrid approaches, including Stokes-vector (SV)-DD receivers [14] and Kramers-Kronig (KK) receivers [15], which were recently proposed and studied extensively. These hybrid schemes can be categorized as advanced direct-detection solutions [16]. These schemes effectively employ complex vector modulation and/or polarization division multiplexing in a self-coherent manner to improve the transmission data rate and distance, and have shown a certain level of potentials as a way to forward in some application scenarios. These advanced DD schemes can be treated as a compromise between the digital coherent and IM/DD solutions, having a clear tradeoff between the transmission performance and system complexity. Since these self-coherent approaches do not strictly follow the conventional definition of the IM/DD system, they are not the focus of this work. Interested readers can refer to [14]-[18], where more details on the topics can be found.

In this paper, we extend our OFC contribution [19] to provide a more detailed overview and outlook of different aspects of current high-speed IM/DD technologies, which are of a great potential to conquer the 200 Gbps/lane milestone for the development of the next-generation client side optical transceivers. The rest of this paper is organized as follows: in Section II, we present a review of recent development of optoelectronic devices with a main focus on the broadband modulators to facilitate high-speed signal modulation. Section III describes the use of different modulation formats together with DSP algorithms for IM/DD system impairment mitigation. We also show our recent works on 200 Gbps/lane IM/DD transmissions as examples and discuss the system performance in that section. In Section IV, a summary of state-of-the-art IM/DD system demonstrations enabled by various key technologies are presented. Finally, we give our conclusions and future outlook in Section V.

II. BROADBAND OPTOELECTRONIC DEVICES FOR HIGH-SPEED MODULATION

For a long period of time, the components for electrical-to-optical and optical-to-electrical conversions, the optoelectronic modulators in particular, have been the bottleneck of end-to-end channel bandwidth in the fiber-optic communication links. This is mainly due to the fact that the design, fabrication and packaging process of optoelectronic components and devices to support broad bandwidth while keeping a low noise level are fundamentally challenging. It requires technology advances in different fields, including material process, design, fabrication and packaging. Recently, there has been a significant progress in the design and manufacturing of such broadband components, which greatly enhance the channel capacity of fiber-optic communication systems. In this section, we focus on four types of commonly used devices, i.e. vertical cavity surface emitting laser (VCSEL), direct modulated laser (DML), Mach–Zehnder modulator (MZM) and electro-absorption modulator integrated with a distributed feedback laser (EA-DFB). The advantages in these devices are among the key enablers for high-speed IM/DD transmissions to support future applications.

VCSEL: Most of today's commercial short-reach (<300 m) intra-datacenter optical links employ GaAs 850 nm multimode (MM) VCSELs combined with MMF. With MM VCSELs, over 30 GHz 3 dB modulation bandwidth was achieved with power consumption of less than hundred femtojoules per bit [20]. Beyond 100 Gbps transmission over tens or hundreds of meters MMF were demonstrated using various modulation formats [21]-[26]. The achievable data rate and distance of the VCSEL and MMF-based scheme are mainly limited by modal dispersion since different transverse modes travel at different propagation velocities in the MMF, resulting in severe inter-symbol-interference (ISI) at the receiver side. The impact of the modal dispersion on the system performance is determined by the number of transverse modes emitted from the VCSEL source and the bandwidth-distance product of the optical fiber, and it can be reduced or eliminated with few-mode or single-mode operation [27]. Therefore, to support emerging hyper-scale datacenters with optical interconnects of 500 m and longer, SMF should be deployed. Correspondingly, it is desirable to adopt single mode (SM) VCSEL, which may support spectrally efficient transmissions over a longer reach compared with the MM VCSEL-based technologies. However, a main drawback is that SM VCSELs often have limited output power and need more complex optical alignment. To rule out the lasing of high-order transvers modes and realize quasi/single mode lasing, one can shrink the aperture size via oxidation [28] or integrate a mode filter generated with a surface relief [29]. Over 100 Gbps per lane transmissions with SM VCSELs operating in the telecom bands were recently reported [30]-[33]. Moreover, within the upper limit of GaAs technology, VCSELs emitting at 980 nm, 1060 nm and 1110 nm have been explored with high modulation bandwidth and a negligible increase in fabrication complexity [34].

DML: As the modulated signal directly drives the laser bias current, DMLs normally emit high output power and is considered a more power- and cost-efficient solution than the external modulation solutions. Additionally, their compactness also facilitates integration with other devices. These merits make DMLs favorable for cost-sensitive datacenter and access networks. However, limited modulation bandwidth often appears as the constraint in extending its potential to provide high-speed data links. Lately, several novel techniques are reported for enhancing the modulation bandwidth of DMLs [35], including multiple quantum wells (MQWs) laser design [36], multi-section laser design [37], and injection locking [38]. With the multi-section laser design, a state-of-the-art DML with 55 GHz modulation bandwidth was reported, which enables a single lane of 112 Gbps 4-level pulse amplitude modulation (PAM-4) transmission without any off-line equalization [39]. Furthermore, by using advanced modulation formats combined with DSP, single channel 100 Gbps transmissions were demonstrated with commercial low-cost 10G-class DMLs [40]. These results indicate the promising potential of DMLs for supporting beyond 200 Gbps/lane applications. Besides the bandwidth limitation, another well-known problem with DML-based system is the DML's inherent chirp effect that broadens the spectrum. Correspondingly, both optical [41], [42] and digital signal processing techniques [43] are proposed to tackle the chirp effect and make a full use to enhance transmission performance [44].

MZM: A commonly used external modulator type for IM/DD optical communications is the MZM, which achieves intensity modulation by combining two phase modulators with a Mach-Zehnder interferometer structure. In order to support high-speed transmissions with advanced modulation formats, there is a growing demand for high-performance and small-size MZMs[45]. Commercial lithium niobite ($LiNbO_3$) MZMs have been used to demonstrate 100 Gbps transmissions and beyond [46]-[48]. However, these commercial components are normally packaged into large-size modules, which are expensive and power hungry, hindering their use for client-side optical interfaces such as the pluggable optical transceivers [49]. Some recent works were reported on designing integrated nanophotonic $LiNbO_3$ MZMs with low voltage and high bandwidth (>100 GHz) [50], [51], and their massive production capabilities remain to be seen. Nowadays, indium phosphide (InP)-based MZMs can be fabricated at low cost, and allow for monolithic integration with a small size. Recently, S. Lange *et al.* presented an InP-based DFB laser monolithically integrated with an MZM of 54 GHz bandwidth [52], [53], and Yamazaki *et al.* demonstrated an InP-based 80 GHz MZM with a capacitance-loaded traveling-wave electrode (CL-TWE) [54]. Another attractive candidate is silicon photonics (SiP)-based MZMs, which can be fabricated using wafer-scale technology compatible with the semiconductor industry. Recently, SiP-based traveling-wave MZM (TW-MZM) [55], [56] and multi-electrode MZM (ME-MZM) [57] have been widely investigated. A detailed review of the development of silicon photonics-based modulator can be found in [58]. Besides the InP and SiP-based MZMs that are already in industrial

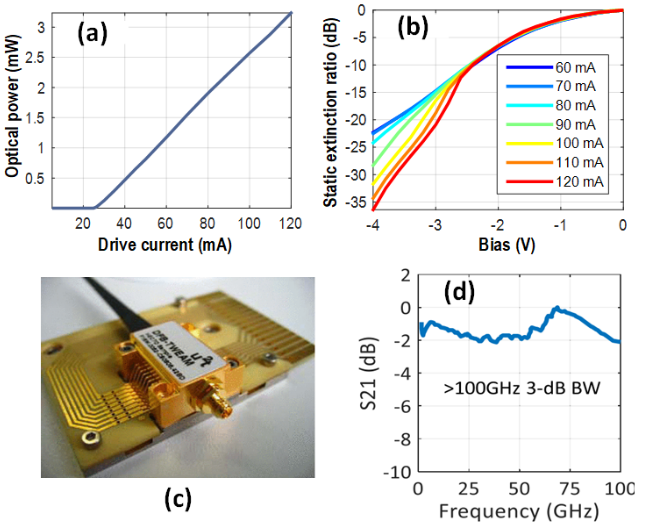

Fig. 2. (a) P(I) characteristics; (b) P(V) characteristics of the DFB-TWEAM module [66]; (c) picture of the packaged module; (d) small-signal transfer characteristics S21 [65].

development stage, recent explorations of silicon-organic hybrid (SOH) MZMs have demonstrated promising properties to support modulation of high data rates [59], [60].

EA-DFB laser: Semiconductor lasers integrated with electro-absorption modulators (EAM) have been manufactured and used in commercial transceivers for 10G and 25G applications. This type of the laser has generally better performance in terms of modulation linearity, extinction ratio and bandwidth compared with the DML [61]. On the other hand, compared with the external MZM, the EA-DFB laser usually has a smaller size, lower driving voltage and potentially lower cost. Therefore, further development and use of this type of the laser for future high-speed transmission applications seem promising. Demonstrations of over 100 Gbps transmissions are reported using EAMs of around 25 GHz bandwidth [62], [63]. EA-DFB laser of >50 GHz modulation bandwidth has been reported supporting high-speed data transmission [64]. One state-of-the-art device of this type is a DFB laser monolithically integrated with a traveling-wave EAM (DFB-TWEAM), which has a 3 dB modulation bandwidth of over 100 GHz [65]. With this device, we have recently demonstrated several high-speed transmission works including [66], [67]. This device was designed by KTH Royal Institute of Technology, fabricated by KTH and Syntune, and packaged by u^{2}t Photonics (currently II-VI/Finisar) [68]. The absorber is based on the 12 strain compensated InGaAsP quantum wells/barriers (QWs) of around 9 nm thickness each. The gain section of the DFB is based on 7 QWs 7 nm thick grown by metal vapor-phase epitaxy (MOVPE) coupled with butt-joint technique on n-doped InP substrate. Figures 2 (a) and (b) show the P(I) and P(V) characteristics of the DFB-TWEAM [66]. A picture of the packaged device is shown in Fig. 2 (c). In Fig. 2(d), the small signal transfer response of the TWEAM is displayed, where 3 dB bandwidth beyond 100 GHz with less than 2 dB ripple in the passband can be observed [65]. It is worth noting that this DFB-TWEAM device was used for a real-time transmission system demonstration of a 100 Gbps non-return to zero (NRZ) on-off-keying (OOK) signal without using any pre- or post-signal processing during the EU FP6 HECTO Project [69]. In this demonstration, the modulated signal showed negligible distortion compared with the electrical driving signal, evincing both broad bandwidth and high linearity of the phase response of the DFB-TWEAM device.

III. MODULATION FORMATS, DSP AND PERFORMANCE

For IM/DD transceivers supporting up to 100 GbE traffic, the NRZ OOK modulation format has been employed with a data rate of up to 25 Gbps/lane [6]. For the forthcoming transition to 400 GbE, a straightforward upgrade from NRZ OOK to PAM-4 is adopted by the IEEE 400GbE 802.3bs standard [70]. For future applications beyond 400G, the options for the modulation format to support 100/200 Gbps per lane are still open for discussion. Among different options, the high level PAM and discrete multitone (DMT) are the two main candidates, which attract much attention. Hence, they are selected for detailed discussions in the remaining of this section. We present our experimental investigations on using these two modulation formats to approach 200 Gbps/lane transmissions [71]-[73]. Besides the PAM and DMT, it is worth mentioning that other modulation formats, including carrier-less amplitude and phase (CAP) modulation [74],[75] and half-cycle subcarrier modulation (SCM) [76] (though not elaborately covered in this paper) have also been investigated and demonstrated experimentally with over 100 Gbps/lane data rates.

A. PAM

The PAM is a modulation format that encodes binary data into multi-level signal pulses, and its simplest 2-level form is the NRZ OOK in the context of IM/DD communications. Employing the PAM signal with a higher number of amplitude levels enables higher system spectral efficiency. On the other hand, higher-level PAM signal sets the stricter requirement for system signal-to-noise ratio (SNR). This is because for a N-level PAM signal (PAM-N, N>2), its eye height is reduced by a factor of (N-1) compared to that of NRZ OOK, given the same signal amplitude peak-to-peak [77], [78]. To increase the system bitrate, one can either increase the signal bandwidth by using a higher symbol rate, or increase the spectral efficiency by using higher order of modulation formats. The former approach requires an upgrade of the end-to-end system bandwidth, including all the bandwidth-limited optical and electrical components. This, in turn, requires an upgrade of design and fabrication technologies for devices and materials. The latter approach requires a system with large effective number of bits (ENoB) from end to end, and often can be used to achieve a higher lane rate without replacing all the bandwidth-limiting components of a deployed IM/DD system. In addition, DSP algorithms and forward-error-correction (FEC) coding can be used to improve the transmission performance.

Feedforward equalizer (FFE) and decision-feedback equalizer (DFE) are two commonly used equalizer structures for PAM signals [79]. FFE consists of a number of taps with

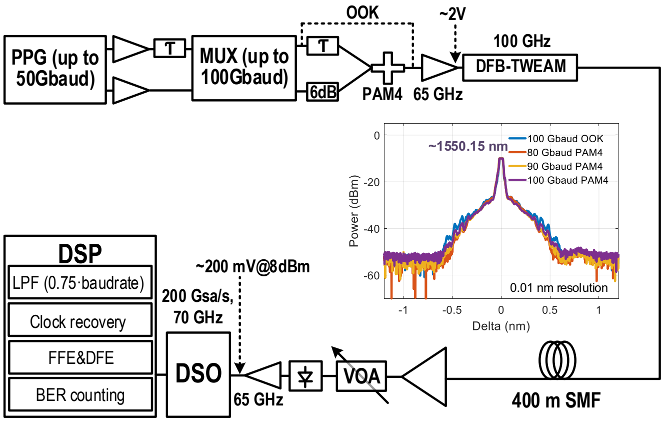

Fig. 3. Experimental configuration of up to 100 Gbaud PAM-4 transmission. PPG: pulse pattern generator; MUX: multiplexer; VOA: variable optical attenuator; DSO: digital storage oscilloscope; LPF: low-pass filter. Inset: optical spectra of the modulated signal at transmitter.

impulse response determined by the tap weights. The tap weights can be adapted by several different algorithms, e.g. decision-directed least-mean-square (LMS) algorithm or recursive least squares (RLS) algorithm. In terms of implementation, one can use either symbol spaced or fractionally spaced FFE configuration, i.e. the FFE operates at 1 sample per symbol (SPS) or > 1 SPS. By minimizing the cost function defined for each algorithm, the FFE eventually converges to a state when the equalizer response represents the inverse of the channel frequency response. It is known that in a bandwidth-limited system the FFE boosts the high frequency signal components and minimizes the ISI. Nevertheless, the high-frequency noise can be enhanced, which may degrade the overall performance for the case of a limited modulation dynamic range. To address such drawback of FFE, DFE can be employed, which utilizes the post-decision symbols for cost function reduction. The implementation of DFE is often combined with the FFE by adding the decision feedback loop with symbol-spaced taps to suppress the high-frequency noise induced by the FFE, and to effectively compensate for both the pre-cursor and post-cursor ISI. Such a configuration shows superior equalization performance compared with that of solely using the FFE. However, it suffers from a decision delay and may also cause error propagation problem due to erroneous decisions. Therefore, when selecting an optimal equalizer type for a transceiver design, one needs to consider both the transceiver specifications and the aimed application scenario.

We have experimentally explored the potential of using FFE and DFE for 200 Gbps/lane IM/DD transmissions with PAM-4, and our experimental setup is shown in Figure 3 [71]. At the transmitter side, an electrical NRZ OOK signal of up to 100 Gbaud was generated by a multiplexer, and up to 100 Gbaud electrical PAM-4 signal was formed by combining two streams of decorrelated NRZ OOK signals. The DFB-TWEAM device reviewed in Sec. II was used for intensity modulation. The optical spectra of the DFB-TWEAM output for different modulations are shown in the inset of Fig. 3. At the receiver, the received signal is sampled at 200 GSa/s at the real-time digital storage oscilloscope (DSO), and then down sampled to 1 SPS after clock recovery. A combination of FFE and DFE is used to equalize the signal. Both the FFE and the DFE operate at 1 SPS in order to cover the sufficient memory length due to the pulse broadening induced by filtering and the fiber chromatic dispersion (CD). In Figure 4, we show quantitative and qualitative measures for up to 100 Gbaud OOK and PAM-4 signals for back to back (b2b) and 400-m SMF transmission. The bit-error-rate (BER) results as a function of received power for different equalizer configurations are shown in Fig. 5(a). For the analysis purposes, hard-decision (HD)-FEC code with 7% and 20% overhead (OH) and soft decision FEC (SD-FEC) with 20% OH are considered (pre-FEC BERs at 5×10^{-3} [80], 1.1×10^{-2} [81] and 2×10^{-2}, respectively). The SD-FEC is considered due to poor electrical b2b signal quality suffered from the implementation penalty. The BER curves are obtained using a 9-feedforward (FF)-tap and 9-feedback (FB)-tap symbol-spaced DFE for the OOK, while 71-FF-tap and 15-FB-tap DFE are implemented for PAM-4. Figs. 5(b)-(d) show the eye diagrams and histograms of the OOK and PAM-4 signals with and without equalizations. In the case of the OOK, BER performance of below the 7% HD-FEC limit for both optical b2b and 400-meter transmission was achieved. From the PAM-4 results, several messages can be extracted when compared with OOK: 1) a severer degradation due to high sensitivity requirements and poor electrical signal performance at the transmitter; 2) a significant increase of the equalizer tap number is needed to reduce the impact of the electrical

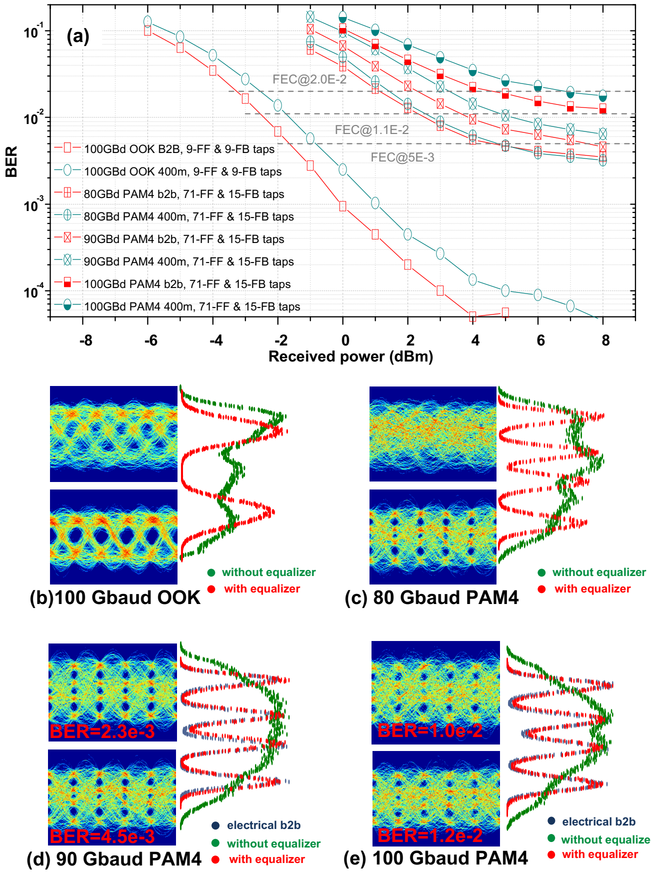

Fig. 4. (a) BER curves for the OOK and PAM-4 signals for b2b and 400 meters, (b)-(c) eye diagram and histograms at optical b2b without and with DFE at 8 dBm, and (d)-(e) eye diagrams and histograms with DFE for electrical b2b (top) and optical b2b (bottom) at 8 dBm.

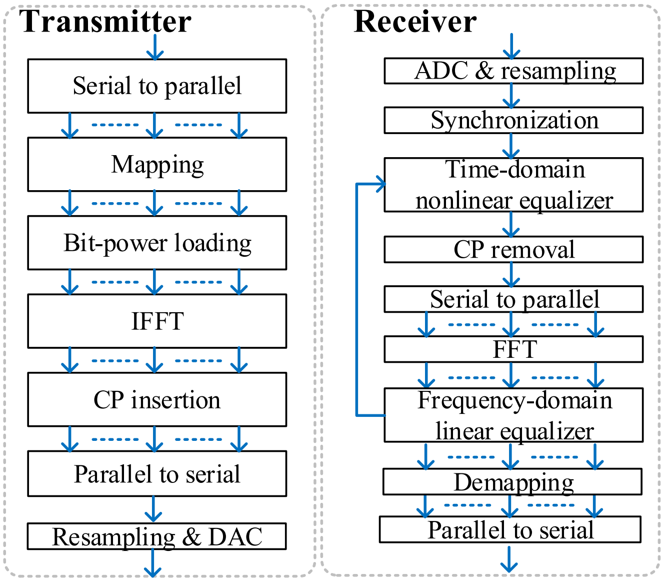

Fig. 5. A typical DSP routine of the DMT transmitter and receiver. FFT / IFFT: fast Fourier transform / inverse FFT; CP: cyclic prefix.

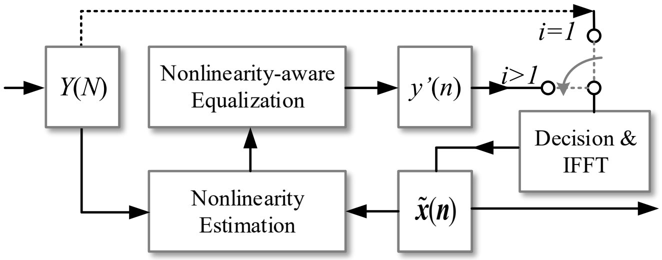

Fig. 6. The structure of the time-domain nonlinear equalizer.

components on the PAM-4 signals; and 3) a larger overhead of FEC is needed, in particular when increasing the baud rate. Improvement in the performance can be confidently expected with a better-quality electrical driving signal and more advanced DSP algorithms. For instance, the maximum likelihood sequence estimation (MLSE) function has been used to effectively enhance the performance of bandwidth-limited signals [82], [83], and partial-response PAM signals [84]. Moreover, equalizers based on Volterra series can be used to compensate for system nonlinear impairments [85]-[87]. Recently, machine learning (ML)-based equalization techniques, e.g. artificial neural network (ANN) [88]-[92] and support vector machine (SVM) [93], [94] are also proposed and investigated for short-reach IM/DD systems. These advanced equalizers have demonstrated improved performance compared with the conventional FFE/DFE equalizers. Interested readers can refer to [95] for a more detailed review of digital equalizers for PAM signals.

B. DMT

The DMT is a type of frequency division multiplexing (FDM) technique, where the input data sequence is encoded in parallel onto many subcarriers [96]. It is the modulation format originally chosen for the first ITU-T asymmetric digital subscriber line (ADSL) standard [97] and later for the ITU-T very high speed digital subscriber line 2 (VDSL2) standard [98]. Recently, DMT attracted attention for short reach IM/DD systems owing to its intrinsic flexibility to shape the frequency spectrum of the transmitted signal, which can be used to maximize the spectral efficiency through bandwidth-limited channels with bit- and power-loading schemes. For instance, over 10 Gbps real-time IM/DD DMT transmission was demonstrated over 25 km SMF with transmitter and receiver FPGAs operating only at 4GS/s [99]. Unlike single carrier modulation formats, DMT does not perform pre- or post-equalization to flatten the received signal spectrum by suppressing the low-frequency components of the signal. Such an equalization approach sacrifices the overall channel capacity as the low-frequency regime of the modulated signal normally corresponds to a high SNR. Instead, the DMT can first estimate the channel response and calculate the in-band frequency-dependent SNR values with a probe signal through the channel, and then adaptively assign modulation orders and power levels respectively for each subcarrier [100]. An effective and widely adopted bit- and power-loading solution is known as the Chow's algorithm [101]. With the bit- and power- loading, the subcarriers at low-frequency regime can benefit from the high SNR with assignment of higher modulation orders, while subcarriers on the high-frequency roll-off edge can still be used to carry data with lower modulation orders. In such a way, the overall channel bandwidth usage can be maximized. However, similar to other multi-carrier systems, the DMT has its drawbacks such as high peak-to-average power ratio (PAPR). Theoretically, the upper bound of PAPR in a DMT waveform is proportional to the number of subcarriers [102]. This circumstance imposes a performance trade-off between spectral granularity of the DMT subcarriers and the required resolution of digital-to-analog converters (DAC) and analog-to-digital converters (ADC). Additionally, DMT with a high PAPR are less tolerant to the relative intensity noise (RIN) compared with PAM [103].

In order to optimize the efficiency of the DAC and ADC with limited ENoB, the signal waveform is often actively clipped. It is also common to drive the optical modulators in the nonlinear region to guarantee a high modulation index, and, hence, to maximize the achievable system SNR. This is particularly important for high spectrally efficient signals when the SNR is a limiting factor. However, enhanced system nonlinearities occur when the transmitter-induced nonlinearities interplay with the fiber CD and the nonlinear square-law detection at the receiver. Therefore, nonlinear equalizers at the receiver can be used to mitigate such nonlinear distortions and improve the overall transmission performance, which was verified in our recent experiment with a high-speed C-band DMT transmission system [73]. Figure 5 shows a typical DSP routine of the DMT transmitter and receiver that we employed for our experiment. On the transmitter side, the bit- and power-loading technique was used in addition to conventional DSP blocks to encode the subcarriers and generate the DMT waveform. At the receiver, a time domain nonlinear equalizer (TD-NE) was used to mitigate system nonlinearities. To reduce complexity, a simplified nonlinear model was suggested which takes into consideration the 2nd-order and partially 3rd-order terms of the Volterra series model to mitigate the nonlinearity components with

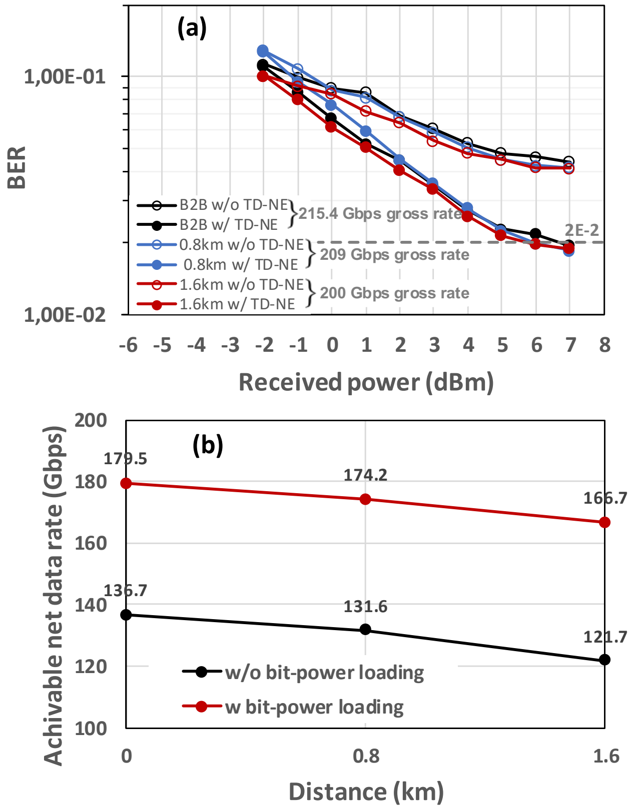

Fig. 7. (a) BER performance of the DMT signals for b2b and up to 1.6-km transmissions with and without the time-domain nonlinear equalizer, (b) achieved net data rate as a function of transmission distance.

certain channel memories [104]. The DSP structure of the employed TD-NE is shown in Fig. 6. The signal is first equalized by a frequency domain one-tap linear equalizer before feeding back to the TD-NE block. The input to the TD-NE is denoted as $Y(N)$ and its corresponding time domain sample is $y(n)$. In the first iteration, $Y(N)$ is fed to a decision-feedback (DF) function followed by an inverse fast Fourier transform (IFFT) module to get the estimation of the transmitted temporal samples $y(n)$, denoted as $\tilde{x}(n)$. The nonlinear kernels are estimated by comparing $y(n)$ with $\tilde{x}(n)$. The estimation process is realized by a data-aided RLS algorithm. Upon its convergence, we can obtain the nonlinear kernels. The signal is then equalized by subtracting the reconstructed nonlinear noise components. After this iteration, the equalized signal $y'(n)$ is utilized as an input for the DF module for the next iteration. The performance is initially improved with a number of iterations until the improvement becomes saturated. In [73] it is observed that the improvement saturation occurs after the 3rd iteration.

The experimental setup for our DMT transmission study is similar to the one shown in Fig. 3 except for the transmitter and fiber link configurations. At the transmitter, a 92 GSa/s arbitrary waveform generator (AWG) is used to generate the signal drive the DFB-TWEAM, and the fiber link consists of up to 1.6 km SMF. For each tested link distance, we set the received optical power to maximum (+7 dBm in all test cases), and then iteratively optimize the parameters of the bit- and power-loading algorithm and the corresponding parameters of the TD-NE to obtain a maximum achievable gross data rate with a stable performance of a BER level below the 20% OH SD-FEC limit. In our experiment, the gross date rates after the bit- and power-loading are 215.4 Gbit/s, 209 Gbit/s, and 200 Gbit/s for the three tested cases, respectively [73]. Figure 7(a) shows the measured BER curves of the received DMT signals of the maximum gross data rates with and without the TD-NE. Significant performance improvement can be observed after mitigating the nonlinear impairments compared with the cases without TD-NE shown in Fig. 7(a). A longer distance causes an obvious reduction on the maximum achievable data rate. The achievable net data rates for different distances with and without bit- and power-loading are shown in Fig. 7(b). It can be seen that bit-power loading can significantly improve the net rate (increase by 30-40%). With the work shown in Fig. 7 as a benchmark, further performance improvement in the achievable transmission distance and data rate can be expected. In terms of the transmission distance, the SMF attenuation in the C-band is at a minimum, whereas the fiber CD induces the well-known small-signal transfer function, i.e. the power fading notches at certain frequencies for double sideband (DSB) modulated signals. This results in the end-to-end channel bandwidth limit, and consequently generates penalty. One straightforward approach is to shift the transmission window to the O-band where dispersion is minimized [40]. Single sideband (SSB) or vestigial side-band (VSB) DMT configurations in this case can be used to overcome such limitations and is demonstrated to improve the transmission distance [105], [106]. With respect to improving achievable data rate, the bottleneck lies within the electrical signal source, as the 3 dB analog bandwidth of the DAC is limited, which is much smaller compared with the bandwidth of the electro-optic modulator (e.g. DFB-TWEAM in [65]). Therefore, an improved electrical signal source, e.g. a DAC with high resolution and/or broader analog bandwidth can potentially unlock the bandwidth bottleneck and improve the system capacity. To date, there have been a number of record demonstrations exceeding 200 Gbps/lane milestone with different key technologies from different aspects, which are summarized in the following section.

IV. Recent Advances for Beyond 200 Gbps per Lane IM/DD Transmissions

There are technical challenges in almost every segment of the IM/DD system when the single lane data rate demand goes beyond 200 Gbps. Meanwhile, we have also been witnessing tremendous research and development efforts and significant technical breakthroughs in high-speed DAC/ADC technologies, novel optoelectronic components and devices, advanced modulation, coding and DSP techniques, since only a few years back. Along with these advances, there have already been a number of system-level demonstrations reporting line rates of beyond 200 Gbps per lane IM/DD transmissions. In this section, we summarize the state-of-the-art IM/DD transmission works and review the key enabling technologies, aiming to provide an overall picture of the frontline in this research direction.

Table I summarizes and compares various IM/DD

TABLE I
SUMMARY OF RECENT IM/DD ACHIEVEMENTS WITH LINE RATE OF 200 GBPS PER LANE AND ABOVE

Modulator device	λ Band	Line rate (Gbps)	Modulation format	Link	Key techniques	FEC limit	Ref.
59-GHz LE-EA-DFB	O-band	214	PAM-4	10-km SMF	FFE	3.8E-3	[107] [108]
59-GHz LE-EA-DFB	O-band	300	DMT	10-km SMF	AMUX	2.63E-2	[109] [110]
80 GHz InP TWMZM	C-band	400.16	DMT	20-km SMF + DCF	AMUX, Volterra	2.7E-2	[54]
30-GHZ MZM	C-band	214/200	PAM-4	b2b/0.5-km SMF	SP-DAC, MLSD	3.8E-3	[111][112]
100-GHz DFB-TWEAM	C-band	200	PAM-4	0.4-km SMF	DFE	2E-2	[71]
100-GHz DFB-TWEAM	C-band	209/200	DMT	0.8-km / 1.6-km SMF	TD-NE	2.7E-2	[72][73]
54-GHz DFB-MZM InP PIC	C-band	200/300	PAM-4/PAM-8	1.2-km SMF	FDE, LUT	3.8E-3/1.9E-2	[49][53]
100-GHz DFB-TWEAM	C-band	204	OOK	10-km SMF +DCF	LUT, MAP	5E-3	[113][114]
40-GHz MZM	C-band	200	PAM-4	40-km SMF + DCF	1-to-4 SiGe HBT BiCMOS ADC, Volterra	3E-4	[115]
>65-GHz CC-SOH-MZM	C-band	200	PAM-4	b2b	Pre-compensation	1E-2	[116]
30-GHz MZM	C-band	244/216	DMT	1-km / 2-km SMF	TCM, Volterra	4.5E-3	[117]
32-GHz MZM	C-band	225	DB-PAM-6	b2b	NL-MLSE	3.7E-3	[118]
22.5-GHz SiP TW-MZM	C-band	200	PAM-6	b2b	MLSD	1.5E-2	[119]
30-GHz MZM	C-band	205/240	DB-PAM-8/ 3D-DB-PAM-8	b2b	TCM, Volterra	4E-3	[120]
40-GHz EML	C-band	260	PS-PAM-8	1-km NZDSF	Pre-EQ, clipping	2E-2	[121]
33GHz MZM	C-band	222	THP-PAM-8	2-km SMF	FTN, THP, FFE	2E-2	[122][a]
30-GHz DDMZM	O-band	255/240	PAM-8	b2b / 2-km MCF	NL-MLSE	3.8E-3	[123]
40-GHz EML	C-band	204.75	PAM-8	1-km SMF	FFE, LUT, ANF	2.7E-2	[124]

[a] Results are not included in the paper but presented at the conference.

transmission demonstrations with line rates of 200 Gbps per lane and beyond. To the best of our knowledge, the first demonstration breaking this borderline was reported back in 2016, where Kanazawa *et al.* achieved a 214 Gbps PAM-4 transmission by using an O-band lumped-electrode electro-absorption modulator integrated with a distributed feedback laser (LE-EADFB) with a 3 dB bandwidth over 59 GHz [107], [108]. With the same laser module, a 300 Gbps DMT transmission was reported by further extending the driving signal bandwidth with a digital-preprocessed analog multiplexed DAC (DP-AM-DAC) and an analog multiplexer (AMUX) [109], [110]. In the latest achievement from the same group, a line rate of 400 Gbps DMT transmission was demonstrated, by using the 80-GHz MZM with CL-TWE, as mentioned in Sec. II, which was wire-bonded to the AMUX [54]. In [111] and [112], an in-house fabricated selector power digital-to-analog converter (SP-DAC) was used to demonstrate up to 214 Gbps PAM-4 generation and 200 Gbps transmission over 0.5 km SMF in the C-band, with the assistance of a maximum likelihood sequence detection (MLSD) at the receiver. Besides the transmission works with PAM-4 and DMT that are presented in Sec. III, the DFB-TWEAM was also employed for a 204 Gbaud OOK transmission, where two 2:1 InP DHBT multiplexing selector was used to generate the high-baud rate OOK signal [113], [114]. A maximum a posteriori (MAP) symbol detector with a look-up-table (LUT) at the receiver was used in this work to detect the received symbols. On the receiver hardware, a 1-to-4 SiGe HBT BiCMOS ADC was reported, which was used for a 200 Gbps PAM-4 transmission over 40 km SMF with only 14 GHz of ADC bandwidth [115]. In a very recent work, a capacity coupled SOH modulator with 3 dB bandwidth above 65 GHz was employed for an optical b2b 200 Gbps PAM-4 demonstration [116]. It is worth noting that this work only has pre-compensation at the transmitter but no post-processing, indicating the end-to-end system with a broad bandwidth and high linearity.

Besides the novel design and development in the device domain, advanced modulation, coding and DSP schemes represent another way to further push forward the line rate even with limited system bandwidth. With respect to modulation formats, the Trellis coding modulation (TCM)-assisted DMT [117] and PAM [118]-[120] signals were used to optimize the Euclidean distances between bits or symbols, thus to improve the overall system performance. Besides, probabilistic-shaped (PS) PAM-8 signal was employed for a demonstration of up to 260 Gbps C-band transmission [121]. In terms of novel equalization techniques, transmitter-side pre-equalization using the Tomlinson-Harashima precoding (THP) can effectively avoid the error propagation problem in the DFE, and it can be combined with the other post-equalization schemes to maximize channel efficiency [122]. Novel post-compensation algorithms including nonlinear (NL)-MLSE [123], and adaptive notch filter (ANF) [124] were also proposed and employed to demonstrate beyond 200 Gbps IM/DD transmissions, showing a great potential to overcome the system bandwidth limitations. Interested readers can refer to the original papers listed in Table I for technical details.

V. CONCLUSIONS AND OUTLOOK

We made an overview the state-of-the-art technologies in devices, modulation formats, and DSP algorithms that can potentially enable 200 Gbps per lane IM/DD system development. Novel broadband electronics and optoelectronic devices can considerably relax the system bandwidth limitations. Meanwhile, advanced modulation formats, coding, and DSP schemes can improve the system efficiency and transmission performance, to further push forward the single lane rate with given system bandwidth. With such a significant progress during the past years, it is expected that novel technology candidates will converge into feasible solutions to fulfill the requirements for future high-speed client-side optics, where IM/DD transmissions are still dominating. On the other hand, the fast development of digital coherent technologies has been pushing towards short-reach scenarios and closing the gap of cost, power consumption, and a packaging size. Advanced direct detection systems with SV-DD or KK schemes are also pushing the limitations ahead to find their way for industrial development. Nevertheless, fundamental research in continuing driving the traditional IM/DD technologies to the higher speed will remain an important task in the field of fiber-optic communications, and such research efforts will also eventually benefit other advanced technology alternatives in the long-term perspective.

REFERENCES

[1] H. Sun, K-T. Wu, and K. Roberts, "Real-time measurements of a 40 Gb/s coherent system," *Opt. Express,* vol. 16, pp. 873-879, 2008.

[2] P. J. Winzer, "Beyond 100G Ethernet," *IEEE Commun. Mag.*, vol. 48, no. 7, pp. 26-30, July 2010.

[3] C. Cole, "Beyond 100G client optics," *IEEE Commun. Mag.*, vol. 50, no. 2, pp. s58-s66, February 2012.

[4] C. Kachris, K. Kanonakis and I. Tomkos, "Optical interconnection networks in data centers: recent trends and future challenges," *IEEE Commun. Mag.*, vol. 51, no. 9, pp. 39-45, September 2013.

[5] E. Agrell *et al.*, "Roadmap of optical communications," *J. Opt.*, vol. 18, no. 6, pp. 063002, 2016.

[6] IEEE Standard for Ethernet - Amendment 3: Physical Layer Specifications and Management Parameters for 40 Gb/s and 100 Gb/s Operation over Fiber Optic Cables," pp. 1-172, 27 March 2015.

[7] CFP Multi-source Agreement Documents, [Online] Available: http://www.cfp-msa.org/documents.html

[8] QSFP-DD Multi-source Agreement Specification, [Online] Available: http://www.qsfp-dd.com/specification/

[9] 400G BiDi Multi-source Agreement, [Online] Available: https://www.400gbidi-msa.org/

[10] 100G Lambda Multi-source Agreement Specifications, [Online] Available: http://100glambda.com/specifications

[11] CWDM8 Multi-Source Agreement Specifications, [Online] Available: https://www.cwdm8-msa.org/

[12] 400ZR Project, [Online] Available: https://www.oiforum.com/technical-work/hot-topics/400zr-2/

[13] K. Zhong *et al.*, "Digital signal processing for short-reach optical communications: a review of current technologies and future trends," *J. Lightw. Technol.,* vol. 36, no.2, pp. 377-400, 2018.

[14] K. Kikuchi and S. Kawakami, "Multi-level signaling in the Stokes space and its application to large-capacity optical communications," *Opt. Express*, vol. 22, pp. 7374-7387, 2014.

[15] A. Mecozzi, C. Antonelli and M. Shtaif, "Kramers–Kronig coherent receiver," *Optica*, vol. 3, pp. 1220-1227, 2016.

[16] A. Li *et al.*, "Advanced Direct Detection Techniques for Next-Generation Short-Reach Applications: Stokes Vector vs. Kramers-Kronig Receiver," in *Proc. SPIE 10947, Next-Generation Optical Communication: Components, Sub-Systems, and Systems VIII,* 1094709, March 2019.

[17] D. Che, C. Sun and W. Shieh, "Optical Field Recovery in Stokes Space," *J. Lightw. Technol.,* vol. 37, no. 2, pp. 451-460, 2019.

[18] M. Chagnon, "Optical Communications for Short Reach," *J. Lightw. Technol.*, vol. 37, no. 8, pp. 1779-1797, 2019.

[19] X. Pang *et al.*, "Beyond 200 Gbps per Lane Intensity Modulation Direct Detection (IM/DD) Transmissions for Optical Interconnects: Challenges and Recent Developments," in *Proc. Opt. Fiber Commun.*, San Diego, CA, USA, Mar. 2019, Paper W4I.7.

[20] E. Haglund *et al.*, "30 GHz bandwidth 850 nm VCSEL with sub-100 fJ/bit energy dissipation at 25–50 Gbit/s," *Electron. Lett.*, vol. 51, no. 14, pp. 1096-1098, 2015.

[21] F. Karinou *et al.*, "112 Gb/s PAM-4 Optical Signal Transmission over 100-m OM4 Multimode Fiber for High-Capacity Data-Center Interconnects," in *Proc. Eur. Conf. Opt. Commun.*, Dusseldorf, Germany, 2016, Paper M2C.2.

[22] J. Lavrencik *et al.*, "Scaling VCSEL-MMF Links to 1 Tb/s Using Short Wavelength Division Multiplexing," *J. Lightw. Technol.*, vol. 36, no. 18, pp. 4138-4145, 2018.

[23] C. Kottke *et al.*, "High speed 160 Gb/s DMT VCSEL transmission using pre-equalization," in *Proc. Opt. Fiber Commun.*, Los Angeles, CA, USA, 2017, Paper W4I.7.

[24] T. Zuo *et al.*, "Single Lane 150-Gb/s, 100-Gb/s and 70-Gb/s 4-PAM Transmission over 100-m, 300-m and 500-m MMF Using 25-G Class 850nm VCSEL," in *Proc. Eur. Conf. Opt. Commun.*, Dusseldorf, Germany, 2016, Paper Th.1.C.2.

[25] S. A. Gebrewold *et al.*, "PAM-8 108 Gbit/s transmission using an 850nm multi-mode VCSEL," in *Proc. Conf. Lasers Electro-Opt.,* San Jose, CA, USA, 2017, Paper CI_4_6.

[26] R. Puerta *et al.*, "107.5 Gb/s 850 nm multi- and single-mode VCSEL transmission over 10 and 100 m of multi-mode fiber," in *Proc. Opt. Fiber Commun.*, Anaheim, CA, USA, Mar. 2016, Paper Th5B.5.

[27] H.-Y. Kao *et al.*, "Comparison of single-/few-/multi-mode 850 nm VCSELs for optical OFDM transmission," *Opt. Express,* vol. 25, pp. 16347-16363, 2017.

[28] N. Ledentsov *et al.*, "850 nm single-mode VCSEL for error-free 60 Gbit / s OOK operation and transmission through 800 m of multi-mode fiber," in *Proc. Opt. Fiber Commun.*, San Diego, CA, USA, Mar. 2019, Paper Th4B.6.

[29] P. Westbergh, A. Larsson, E. Haglund, R. Safaisini, and J. S. Gustavsson, "20 Gbit/s data transmission over 2 km multimode fibre using 850 nm mode filter VCSEL," *Electron. Lett.,* vol. 50, no. 1, pp. 40–42, 2014.

[30] C. Xie *et al.*, "Single-VCSEL 100-Gb/s short-reach system using discrete multi-tone modulation and direct detection," in *Proc. Opt. Fiber Commun.*, Los Angeles, CA, USA, 2015, Paper Tu2H.2.

[31] X. Pang *et al.*, "7×100 Gbps PAM-4 Transmission over 1-km and 10-km Single Mode 7-core Fiber using 1.5-µm SM-VCSEL," in *Proc. Opt. Fiber Commun.*, San Diego, CA, USA, 2018, Paper M1I.4.

[32] L. Zhang *et al.*, "Nonlinearity Tolerant High-Speed DMT Transmission With 1.5-µm Single-Mode VCSEL and Multi-Core Fibers for Optical Interconnects," *J. Lightw. Technol.*, vol. 37, no. 2, pp. 380-388, 2019.

[33] J. Van Kerrebrouck *et al.*, "High-Speed PAM4-Based Optical SDM Interconnects with Directly Modulated Long-Wavelength VCSEL," *J. Lightw. Technol.*, vol. 37, no. 2, pp. 356-362, 2019.

[34] A. Liu *et al.*, "Vertical-cavity surface-emitting lasers for data communication and sensing," *Photon. Res.,* vol. 7, pp. 121-136, 2019.

[35] N. H. Zhu et al., "Directly Modulated Semiconductor Lasers," *IEEE J. Sel. Top. Quantum Electron.*, vol. 24, no. 1, pp. 1-19, 2018.

[36] S. Weisser *et al.*, "Damping-limited modulation bandwidths up to 40 GHz in undoped short-cavity In0.35Ga0.65As-GaAs multiple-quantum well lasers," *IEEE Photon. Technol. Lett.*, vol. 8, no. 5, pp. 608–610, 1996.

[37] O. Kjebon *et al.*, "30 GHz direct modulation bandwidth in detuned loaded InGaAsP DBR lasers at 1.55 µm wavelength," *Electron. Lett.*, vol. 33, no. 6, pp. 488–489, 1997.

[38] E. K. Lau *et al.,* "Strong optical injection-locked semiconductor lasers demonstrating >100-GHz resonance frequencies and 80-GHz intrinsic bandwidths," *Opt. Express*, vol. 16, no. 9, pp. 6609–6618, 2008.

[39] Y. Matsui *et al.*, "55 GHz Bandwidth Distributed Reflector Laser," *J. Lightwave Technol.*, vol. 35, pp. 397-403, 2017.

[40] W. Yan *et al.*, "80km IM-DD Transmission for 100 Gb/s per Lane Enabled by DMT and Nonlinearity Management," in *Proc. Opt. Fiber Commun.*, San Francisco, CA, USA, 2014, Paper M2I.4.

[41] H. Ji *et al.*, "Field demonstration of a real-time 100-Gb/s PON based on 10G-class optical devices," *J. Lightw. Technol.*, vol. 35, no. 10, pp.1914-1921, 2017.

[42] L. Xue *et al.*, "Symmetric 100-Gb/s TWDM-PON based on 10G-Class Optical Devices Enabled by Dispersion-Supported Equalization," *J. Lightw. Technol.*, vol. 36, no. 2, pp. 580-586, 2018.

[43] K. Zhang *et al.*, "Intensity directed equalizer for the mitigation of DML chirp induced distortion in dispersion-unmanaged C-band PAM transmission," *Opt. Express*, vol. 25, no. 23, pp. 28123-28135, 2018.

[44] D. Che, F. Yuan, and W. Shieh, "Towards high-order modulation using complex modulation of semiconductor lasers," *Opt. Express,* vol. 24, 6644-6649, 2016.

[45] A. Dochhan *et al.*, "Solutions for 80 km DWDM systems," *J. Lightwave Technol*., vol. 34, pp. 491–499, 2016.

[46] D. Sadot *et al.*, "Single channel 112Gbit/sec PAM4 at 56Gbaud with digital signal processing for data centers applications," *Opt. Express,* vol. 23, pp. 991-997, 2015.

[47] L. Zhang *et al*., "Beyond 100-Gb/s Transmission Over 80-km SMF Using Direct-Detection SSB-DMT at C-Band," *J. Lightwave Technol.*, vol. 34, no. 2, pp. 723-729, 2016.

[48] S. Yamamoto *et al.*, "92-Gbaud PAM4 Transmission Using Spectral-Shaping Trellis-Coded-Modulation with 20-GHz Bandwidth Limitation," in *Proc. Opt. Fiber Commun.*, San Diego, CA, USA, 2019, Paper W4I.5.

[49] C. Wang *et al.*, "Nanophotonic lithium niobate electro-optic modulators," *Opt. Express*, vol. 26, pp. 1547-1555, 2018.

[50] A. J. Mercante *et al.*, "110 GHz CMOS compatible thin film LiNbO3 modulator on silicon," *Opt. Express,* vol. 24, pp. 15590-15595, 2016.

[51] C. Wang *et al.*, "100-GHz low voltage integrated lithium niobate modulators," in *Proc. Conf. Lasers Electro. Opt.,* San Jose, CA, USA, 2018, Paper SM3B.4.

[52] S. Lange *et al.*, "100 GBd Intensity Modulation and Direct Detection with an InP-based Monolithic DFB Laser Mach-Zehnder Modulator", in *Proc. Opt. Fiber Commun.*, Los Angeles, CA, USA, 2017, Paper Th5C.5.

[53] S. Lange *et al*., "100 GBd Intensity Modulation and Direct Detection with an InP-Based Monolithic DFB Laser Mach–Zehnder Modulator," *J. Lightw. Technol.*, vol. 36, no. 1, pp. 97-102, 2018.

[54] H. Yamazaki *et al*., "IMDD Transmission at Net Data Rate of 333 Gb/s Using Over-100-GHz-Bandwidth Analog Multiplexer and Mach–Zehnder Modulator," *J. Lightw. Technol.,* vol. 37, no. 8, pp. 1772-1778, Apr. 2019.

[55] G. Cong *et al.*, "Silicon traveling-wave Mach–Zehnder modulator under distributed-bias driving," *Opt. Lett.*, vol. 43, pp. 403-406, 2018.

[56] M. Li *et al.*, "Silicon intensity Mach–Zehnder modulator for single lane 100 Gb/s applications," *Photon. Res.*, vol.6, pp. 109-116, 2018.

[57] A. Samani et al., "Experimental parametric study of 128 Gb/s PAM-4 transmission system using a multi-electrode silicon photonic Mach Zehnder modulator," *Opt. Express*, vol. 25, pp. 13252-13262, 2017.

[58] W. Shi *et al.*, "Silicon photonic modulators for PAM transmissions," *J. Opt.*, vol. 20, no. 8, Art. no. 083002, 2018.

[59] J. Leuthold et al., "Silicon-Organic Hybrid Electro-Optical Devices," *IEEE J. Sel. Top. Quantum Electron.*, vol. 19, no. 6, pp. 114-126, Art no. 3401413, 2013

[60] Peter O. Weigel *et al.*, "Bonded thin film lithium niobate modulator on a silicon photonics platform exceeding 100 GHz 3-dB electrical modulation bandwidth," *Opt. Express,* vol. 26, pp. 23728-23739, 2018.

[61] C. H. Cox III, G. E. Betts, and L. M. Johnson, "High-performance, externally modulated analog fiber-optic links," *Optics News,* vol. 15, no. 12, pp. 43-44, 1989.

[62] U. Troppenz *et al.*, "1.3 µm electroabsorption modulated lasers for PAM4/PAM8 single channel 100 Gb/s," in *Proc. Int. Conf. Indium Phosphide Related Mater.*, Montpellier, France, 2014, Paper Th.B2.5.

[63] K. Zhong *et al.*, "Amplifier-Less Transmission of Single Channel 112Gbit/s PAM4 Signal Over 40km Using 25G EML and APD at O band," in *Proc. Eur. Conf. Opt. Commun.*, Gothenburg, Sweden, 2017, Paper P2.SC6.21.

[64] M. A. Mestre *et al.*, "Compact InP-Based DFB-EAM Enabling PAM-4 112 Gb/s Transmission Over 2 km," *J. Light. Technol.*, vol. 34, no. 7, pp. 1572–1578, 2016.

[65] O. Ozolins *et al.*, "100 GHz Externally Modulated Laser for Optical Interconnects," *J. Lightw. Technol.*, vol. 35, no. 6, pp. 1174-1179, 2017.

[66] M. Verplaetse *et al.*, "Real-Time 100 Gb/s Transmission Using Three-Level Electrical Duobinary Modulation for Short-Reach Optical Interconnects," *J. Light. Technol.*, vol. 35, no. 7, pp. 1313–1319, 2017.

[67] R. Lin *et al.*, "Real-time 100 Gbps/λ/core NRZ and EDB IM/DD transmission over multicore fiber for intra-datacenter communication networks," *Opt. Express,* vol. 26, pp. 10519-10526, 2018.

[68] M. Chacinski *et al.*, "Monolithically integrated 100 GHz DFB-TWEAM," *J. Lightw. Technol.*, vol. 27, no. 16, pp. 3410–3415, Aug. 2009.

[69] R. H. Derksen *et al.*, "Cost-efficient high-speed components for 100 gigabit ethernet transmission on one wavelength only: results of the HECTO project," *IEEE Commun. Mag.*, vol. 51, no. 5, pp. 136-144, 2013.

[70] IEEE Standard for Ethernet Amendment 10: Media Access Control Parameters, Physical Layers, and Management Parameters for 200 Gb/s and 400 Gb/s Operation Standard, IEEE 802.3bs-2017, Dec. 2017.

[71] O. Ozolins *et al.*, "100 Gbaud 4PAM Link for High Speed Optical Interconnects," in *Proc. Eur. Conf. Opt. Commun.*, Gothenburg, Sweden, 2017, Paper P2.SC5.6.

[72] X. Hong *et al.*, "200-Gbps DMT Transmission over 1.6-km SSMF with A Single EML/DAC/PD for Optical Interconnects at C-Band." in *Proc. Eur. Conf. Opt. Commun.*, Gothenburg, Sweden, 2017, Paper Th.2.A.5.

[73] L. Zhang *et al.*, "Nonlinearity-aware 200 Gbps DMT transmission for C-band short-reach optical interconnects with a single packaged electro-absorption modulated laser," *Opt. Lett.,* vol. 43, pp. 182-185, 2018.

[74] M. I. Olmedo *et al*., "Multiband Carrierless Amplitude Phase Modulation for High Capacity Optical Data Links," *J. Lightw. Technol.*, vol. 32, no. 4, pp. 798-804, 2014.

[75] T. Zuo *et al.*, "O-band 400 Gbit/s client side optical transmission link," in *Proc. Opt. Fiber Commun.*, San Francisco, CA, USA, 2014, Paper M2E.4.

[76] J.C. Cartledge and A.S. Karar, "100 Gb/s intensity modulation and direct detection," *J. Lightw. Technol.*, vol. 32, no. 16, pp. 2809-2814, 2014.

[77] K. Szczerba *et al.*, "4-PAM for high-speed short-range optical communications," *J. Opt. Commun. Netw.*, vol. 4, no. 11, pp. 885–894, Nov. 2012.

[78] X. Pang *et al.*, "Experimental Study of 1.55-µm EML-Based Optical IM/DD PAM-4/8 Short Reach Systems," *IEEE Photon. Technol. Lett.*, vol. 29, no. 6, pp. 523-526, Mar. 2017.

[79] John G. Proakis, "Adaptive Equalization," in *Digital Communications,* Fourth Ed., New York, NY, USA, McGraw-Hill, 2001, pp. 636-679.

[80] Y. Y. Jian *et al.*, "Iterative hard-decision decoding of braided BCH codes for high-speed optical communication," in *Proc. IEEE Global Commun. Conf.*, Atlanta, GA, USA, 2013, pp. 2376-2381.

[81] N. Cvijetic, *et al.*, "First OpenFlow-based Software-Defined λ-Flow Architecture for Flex-Grid OFDMA Mobile Backhaul over Passive Optical Networks with Filterless Direct Detection ONUs," in *Proc. Opt. Fiber Commun.*, Anaheim, CA, USA, Mar. 2013, Paper PDP5B.2.

[82] F. Karinou, N. Stojanovic, and Z. Yu, "Toward cost-efficient 100G metro networks using IM/DD, 10-GHz components, and MLSE receiver," *J. Lightw. Technol.*, vol. 33, no. 19, pp. 4109–4117, Oct. 2015

[83] K. Zhong *et al.*, "140-Gb/s 20-km Transmission of PAM-4 Signal at 1.3µm for Short Reach Communications," *IEEE Photon. Technol. Lett.,* vol. 16, no. 27, pp. 1757-1760, 2017.

[84] Q. Zhang *et al.*, "Single-lane 180 Gb/s DB-PAM-4-signal transmission over an 80 km DCF-free SSMF link," *Opt. Lett.*, vol. 42, pp. 883-886, 2017.

[85] Y. Gao *et al.*, "112 Gb/s PAM-4 Using a Directly Modulated Laser with Linear Pre-Compensation and Nonlinear Post-Compensation," in *Proc. Eur. Conf. Opt. Commun.*, Dusseldorf, Germany, September 2016, pp. 121-123.

[86] N. Stojanovic, F. Karinou, Q. Zhang and C. Prodaniuc, "Volterra and Wiener Equalizers for Short-Reach 100G PAM-4 Applications," *J. Lightw. Technol.*, vol. 35, no. 21, pp. 4583-4594, 2017.

[87] Q. Zhang *et al.,* "Cost-effective single-lane 112 Gb/s solution for mobile fronthaul and access applications," *Opt. Lett.,* vol. 24, pp. 5720–5723 2016.

[88] J. Estaran *et al.*, "Artificial neural networks for linear and non-linear impairment mitigation in high-baudrate IM/DD systems," in *Proc. Eur. Conf. Opt. Commun.*, Dusseldorf, Germany, 2016, Paper M.2.B.2.

[89] S. Gaiarin *et al.*, "High speed PAM-8 optical interconnects with digital equalization based on neural network," in Proc. of *ACP*, Wuhan, China, 2016, Paper AS1C.1.

[90] C.-Y. Chuang *et al.*, “Convolutional neural network based nonlinear classifier for 112-Gbps high speed optical link,” in *Proc. Opt. Fiber Commun. Conf.*, San Diego, CA, USA, 2018, Paper W2A. 43.

[91] Z. Wan *et al.*, “Nonlinear equalization based on pruned artificial neural networks for 112-Gb/s SSB-PAM4 transmission over 80-km SSMF,” *Opt. Express*, vol.8, pp.10631–10642, 2018.

[92] L. Yi *et al.*, "Machine Learning for 100 Gb/s/λ Passive Optical Network," *J. Lightw. Technol.*, vol. 37, no. 6, pp. 1621-1630, 2019.

[93] G. Chen *et al.*, "Nonlinear Distortion Mitigation by Machine Learning of SVM Classification for PAM-4 and PAM-8 Modulated Optical Interconnection," *J. Lightw. Technol.*, vol. 36, no. 3, pp. 650-657, 2018.

[94] M. Bi *et al.*, "A Powerful Equalizer Based on Modified SVM Classifier Without Nonlinear Kernel Enabled 100-Gb/s NG-EPON System With 10-G Class," *IEEE Access*, vol. 7, pp. 71185-71194, 2019.

[95] H. Zhou *et al.*, “Recent Advances in Equalization Technologies for Short-Reach Optical Links Based on PAM4 Modulation: A Review,” *Appl. Sci.*, vol.9 no. 11, pp. 2342, 2019.

[96] J. A. C. Bingham, "Multicarrier modulation for data transmission: an idea whose time has come," *IEEE Commun. Mag.*, vol. 28, no. 5, pp. 5-14, May 1990.

[97] G.992.1: Asymmetric digital subscriber line (ADSL) transceivers, ITU-T Recommendation G.992.1, 1999.

[98] G.993.2: Very high speed digital subscriber line transceivers 2 (VDSL2), ITU-T Recommendation G993.2, 2019.

[99] R. P. Giddings *et al.,* "Experimental demonstration of a record high 11.25Gb/s real-time optical OFDM transceiver supporting 25km SMF end-to-end transmission in simple IMDD systems," *Opt. Express,* vol. 18, pp. 5541-5555, 2010.

[100] J. M. Tang, P. M. Lane, and K. Alan Shore, "High-Speed Transmission of Adaptively Modulated Optical OFDM Signals Over Multimode Fibers Using Directly Modulated DFBs," *J. Lightwave Technol.*, vol. 24, pp. 429-441, 2006.

[101] P. Chow, J. M. Cioffi, and J. A. C. Bingham, “A practical discrete multi-tone transceiver loading algorithm for data transmission over spectrally shaped channels,” *IEEE Trans. Commun.*, vol. 43, pp. 773-775, 1995.

[102] H. Ochiai and H. Imai, "On the distribution of the peak-to-average power ratio in OFDM signals," *IEEE Trans. Commun.*, vol. 49, no. 2, pp. 282-289, Feb 2001.

[103] K. Zhong *et al.*, "Experimental study of PAM-4, CAP-16, and DMT for 100 Gb/s Short Reach Optical Transmission Systems," *Opt. Express*, vol. 23, pp. 1176-1189, 2015.

[104] X. Hong *et al.*, “1.55-µm EML-based DMT Transmission with Nonlinearity-Aware Time Domain Super-Nyquist Image Induced Aliasing,” in *Proc. Opt. Fiber Commun.*, Los Angeles, CA, USA, 2017, Paper Th3D.3.

[105] D. Pilori, C. Fludger and R. Gaudino, "Comparing DMT Variants in Medium-Reach 100G Optically Amplified Systems," *J. Lightwave Technol.*, vol. 34, no. 14, pp. 3389-3399, 2016.

[106] G. N. Liu *et al.*, "IM/DD Transmission Techniques for Emerging 5G Fronthaul, DCI, and Metro Applications," *J. Lightwave Technol.*, vol. 36, pp. 560-567, 2018.

[107] S. Kanazawa *et al.*, “Transmission of 214-Gbps 4-PAM signal using an ultra-broadband lumped-electrode EADFB laser module,” in *Proc. Opt. Fiber Commun.*, Anaheim, CA, USA, Mar. 2016, Paper Th5B.3.

[108] S. Kanazawa *et al.*, "214-Gb/s 4-PAM Operation of Flip-Chip Interconnection EADFB Laser Module," *J. Lightwave Technol.*, vol. 35, no. 3, pp. 418-422, 2017.

[109] H. Yamazaki, *et al.*, "300-Gbps discrete multi-tone transmission using digital-preprocessed analog-multiplexed DAC with halved clock frequency and suppressed image." in *Proc. Eur. Conf. Opt. Commun.,* Dusseldorf, Germany, 2016, Paper Th3B.4.

[110] H. Yamazaki, *et al.*, "Discrete Multitone Transmission at Net Data Rate of 250 Gb/s Using Digital-Preprocessed Analog-Multiplexed DAC With Halved Clock Frequency and Suppressed Image." *J. Lightw. Technol.,* vol. 35, no. 7, pp. 1300-1306, 2017.

[111] M. A. Mestre et al., “100-Gbaud PAM-4 intensity-modulation directdetection transceiver for datacenter interconnect,” in *Proc. Eur. Conf. Opt. Commun.,* Dusseldorf, Germany, 2016, Paper. M.2.C.2

[112] H. Mardoyan *et al.*, “84-, 100-, and 107-GBd PAM-4 Intensity-Modulation Direct-Detection Transceiver for Datacenter Interconnects,” *J. Lightwave Technol.*, vol. 35, no. 6, pp. 1253–1259, 2017.

[113] H. Mardoyan et al., "204-GBaud On-Off Keying Transmitter for Inter-Data Center Communications," in *Proc. Opt. Fiber Commun. Conf.*, San Diego, CA, USA, 2018, Paper Th4A.4.

[114] J M. Estarán *et al.*, "140/180/204-Gbaud OOK Transceiver for Inter- and Intra-Data Center Connectivity," *J. Lightwave Technol.*, vol. 37, pp. 178-187, 2019.

[115] F. Buchali *et al.*, "A SiGe HBT BiCMOS 1-to-4 ADC frontend supporting 100 GBaud PAM4 reception at 14 GHz digitizer bandwidth," in *Proc. Opt. Fiber Commun.*, San Diego, CA, USA, 2019, Paper Th4A.7.

[116] S. Ummethala *et al.*, "Capacitively Coupled Silicon-Organic Hybrid Modulator for 200 Gbit/s PAM-4 Signaling," in *Proc. Conf. Lasers Electro-Opt.,* San Jose, CA, USA, 2019, Paper JTh5B.2.

[117] L. Zhang *et al.*, “Beyond 200-Gb/s DMT Transmission over 2-km SMF Based on A Low-cost Architecture with Single-wavelength, Single-DAC/ADC and Single-PD,” in *Proc. Eur. Conf. Opt. Commun.*, Rome, Italy, 2018, Paper We1H.1.

[118] N. Stojanovic *et al.*, “210/225 Gbit/s PAM-6 transmission with BER bellow KP4-FEC/EFEC and at least 14 dB link budget,” in *Proc. Eur. Conf. Opt. Commun.*, Rome, Italy, 2018, We1H.5.

[119] F. Zhang *et al.*, "Up to single lane 200G optical interconnects with silicon photonic modulator," in *Proc. Opt. Fiber Commun.*, San Diego, CA, USA, 2019, Paper Th4A.6.

[120] C. Prodaniuc *et al.*, “3-Dimensional PAM-8 modulation for 200 Gbps/lambda optical systems,” *Opt. Commun.*, vol. 435, pp. 1–4, 2019.

[121] J. Zhang *et al.*, "Demonstration of 260-Gb/s Single-Lane EML-Based PS-PAM-8 IM/DD for Datacenter Interconnects," in *Proc. Opt. Fiber Commun.*, San Diego, CA, USA, 2019, Paper W4I.4.

[122] Q. Hu *et al.*, "84 GBd Faster-Than-Nyquist PAM-4 Transmission Using Only Linear Equalizer at Receiver," in *Proc. Opt. Fiber Commun.*, San Diego, CA, USA, 2019, Paper W4I.2.

[123] A. Masuda *et al.,* "255-Gbps PAM-8 Transmission under 20-GHz Bandwidth Limitation Using NL-MLSE Based on Volterra Filter,” in *Proc. Opt. Fiber Commun.*, San Diego, CA, USA, 2019, Paper W4I.6.

[124] F. Li *et al.*, "200 Gbit/s (68.25 Gbaud) PAM8 Signal Transmission and Reception for Intra-Data Center Interconnect," in *Proc. Opt. Fiber Commun.*, San Diego, CA, USA, 2019, Paper W4I.3.